

Experimental Quantum Learning of a Spectral Decomposition

Michael R. Geller,^{1,*} Zoë Holmes,² Patrick J. Coles,^{3,4} and Andrew Sornborger^{2,4,†}

¹*Center for Simulational Physics, University of Georgia, Athens, Georgia 30602, USA*

²*Information Sciences, Los Alamos National Laboratory, Los Alamos, NM, USA.*

³*Theoretical Division, Los Alamos National Laboratory, Los Alamos, NM, USA.*

⁴*Quantum Science Center, Oak Ridge, TN, 37931, USA.*

Currently available quantum hardware allows for small scale implementations of quantum machine learning algorithms. Such experiments aid the search for applications of quantum computers by benchmarking the near-term feasibility of candidate algorithms. Here we demonstrate the quantum learning of a two-qubit unitary by a sequence of three parameterized quantum circuits containing a total of 21 variational parameters. Moreover, we variationally diagonalize the unitary to learn its spectral decomposition, i.e., its eigenvalues and eigenvectors. We illustrate how this can be used as a subroutine to compress the depth of dynamical quantum simulations. One can view our implementation as a demonstration of entanglement-enhanced machine learning, as only a single (entangled) training data pair is required to learn a 4×4 unitary matrix.

Quantum simulation and machine learning are among the most promising applications of large-scale quantum computers. Of these, the discovery of algorithms with provable exponential speedup has been more challenging in the machine learning domain, in part because it is harder to port established machine learning techniques to the quantum setting [1]. Notable exceptions include linear system solvers [2–4], kernel methods [5, 6], and Boltzmann machines [7, 8]. But quantum simulation demonstrations [9–13] appear to be ahead of machine learning [14–20] in terms of the maximum problem sizes achieved, suggesting that quantum simulation might yield the earliest applications with quantum advantage.

Variational quantum algorithms [21–23] will likely facilitate near-term implementations for these applications. Such algorithms employ a problem-specific cost function that is evaluated on a quantum computer, while a classical optimizer trains a parameterized quantum circuit to minimize this cost.

Some variational quantum algorithms have interest beyond their ability to achieve quantum advantage on their own, and can serve as subroutines for larger quantum algorithms. These include quantum autoencoders for data compression [24, 25] and linear algebra methods [26–28]. A common subroutine is the training of a variational quantum state to approximate the ground state of a given n -qubit Hamiltonian, which can be the Hamiltonian of a simulated model [29] or some other optimization objective [30–32]. Variational quantum algorithms to learn and diagonalize density matrices have also been developed [33–35], which is a fundamental subroutine that will have many uses including principal component analysis and estimation of quantum information quantities [36, 37]. Another subroutine is the learning of one quantum state by a second state, where the output of a variational circuit is optimized to maximize the over-

lap with an input state that might itself be the output of another algorithm [38–41]. Although a minimum of $2(2^n - 1)$ real parameters are required to do this exactly in general, it is widely believed that for many cases of interest a polynomial number of parameters will suffice.

Beyond learning states, it is also useful to *variationally learn a unitary channel* $\rho \mapsto U\rho U^\dagger$. This is more challenging because now all of the $4^n - 1$ matrix elements must match for an exact replica V of an arbitrary U , up to a global phase. A hybrid protocol for learning a unitary is provided by the quantum-assisted quantum compiling algorithm [38]. This is a low-depth subroutine appropriate for both near-term and fault-tolerant quantum computing.

Given a target unitary U and parameterized unitary $V(\theta)$, both acting on n -qubits, quantum-assisted quantum compiling uses a maximally entangled Bell state on $2n$ qubits to compute the Hilbert-Schmidt inner product, $|\text{Tr}(UV(\theta)^\dagger)|$. Since this inner product is directly related to the average fidelity between states acted on by U and $V(\theta)$ [42, 43], this allows the action of U on all possible input states to be studied using a single entangled input state. Consequently, with this entanglement-enhanced learning strategy, only a single training state is needed to fully learn U , in contrast to the $\sim 2^n$ input-output pairs that are required in the absence of entanglement [44, 45].

Although more challenging than state learning, learning a unitary can be used for a wide variety of quantum information applications, including circuit depth compression, noise-tailoring, benchmarking, and the ‘black box uploading’ of an unknown experimental system unitary [38]. Quantum-assisted quantum compiling has been demonstrated on 1+1 qubits, where a single-qubit variational circuit $V(\theta)$ learned the value of a single-qubit unitary U [38].

Quantum-assisted quantum compiling can be gener-

alized to learn not only a unitary, but also its Schur decomposition $W(\theta)D(\gamma)W(\theta)^\dagger$, where $W(\theta)$ is a parameterized unitary and $D(\gamma)$ is a parameterized diagonal unitary. That is, one can use quantum-assisted quantum compiling to *variationally diagonalize a unitary*. This is useful for a variety of quantum information science applications, since access to the spectral decomposition of a unitary U enables arbitrary powers of U to be implemented using a fixed depth circuit. Specifically, suppose we learn the optimum parameters θ_{opt} and γ_{opt} such that $U = W(\theta_{\text{opt}})D(\gamma_{\text{opt}})W(\theta_{\text{opt}})^\dagger$. We can then implement U^k using the fixed depth circuit $W(\theta_{\text{opt}})D(k\gamma_{\text{opt}})W(\theta_{\text{opt}})^\dagger$. We stress that the parameter k here can take any real value and hence this approach can be used to implement non-integer and negative powers of U .

One important application of variational unitary diagonalization is quantum simulation. Let U be a Trotterized (or other) approximation to a short-time evolution $e^{-iH\Delta t}$ by some Hamiltonian H . We assume that H is local [46–49], sparse [50–52], or given by a linear combination of unitaries [53–55], permitting efficient simulation with bounded error. Then $WD^{t/\Delta t}W^\dagger$ is an approximate *fast-forwarded* evolution operator with a circuit depth that is independent of t . By contrast, most of the best known Hamiltonian simulation algorithms [49, 52, 55] have depths scaling at least linearly in t , inhibiting long time simulations on near-term hardware.

This low-depth algorithm, called variational fast-forwarding [56], lies at an exciting intersection of machine learning and quantum simulation and is an promising approach in the burgeoning field of variational quantum simulation [57–68]. Variational fast-forwarding has been demonstrated on 1+1 qubits [56]. Refinements of variational fast-forwarding for simulating a given fixed initial state [67] and for learning the spectral decomposition of a given Hamiltonian [68] have also been proposed. It is important to note that the unitary being diagonalized need not already be known. Therefore, variational unitary diagonalization could also be used to perform a ‘black box diagonalization’ of the dynamics of an unknown experimental system. Thus, this approach provides a new algorithmic tool for probing dynamics in an experimental setting.

In this work we use `ibmq_bogota` to demonstrate the successful learning of a spectral decomposition on 2+2 qubits. Specifically, we diagonalize the short time evolution unitary for an Ising spin chain. After only 16 steps of training by gradient descent, the spectral decomposition is used to fast-forward the evolution of the Ising model, resulting in a dramatic reduction of simulation error compared with Trotterized Hamiltonian simulation and a significant ($\sim 10\times$) increase in the effective quantum volume of the simulation.

METHODS

Learning task. We demonstrate the variational learning of the spectral decomposition of a unitary by learning a diagonalization of the short-time evolution operator of the 2-spin Ising model

$$H = J \sum_{i=1,2} Z_i Z_{i+1} + B \sum_{i=1,2} X_i. \quad (1)$$

Here J quantifies the exchange energy, B is the transverse field strength and Z_i and X_i are Pauli operators on the i_{th} qubit. We approximate the short-time evolution $\exp(-iH\Delta t)$ of the spin chain using a second order Trotter approximation, that is we take

$$U = \left[\prod_i R_x(\theta_B)_i \times \prod_i R_{zz}(\theta_J)_{i,i+1} \times \prod_i R_x(\theta_B)_i \right]^2 \quad (2)$$

where $\theta_B = B\Delta t/2$ and $\theta_J = 2J\Delta t/2$. The simulated Ising model parameters are listed in Table I. The specific circuit we used for U is shown in Fig. 1.

TABLE I. Ising model parameters.

	Parameter	Value
N	number spins	2
Δt	short evolution time	0.2
J	exchange energy	1
B	transverse field	1

Ansatz. To learn the spectral decomposition of U we variationally compile it to a unitary with a structure of the form

$$V(\theta, \gamma) = W(\theta)D(\gamma)W(\theta)^\dagger, \quad (3)$$

where W is an arbitrary unitary, D is a diagonal matrix and θ and γ are vectors of parameters. After successful training, D will capture the eigenvalues of U , and W will capture the rotation matrix from the computational basis to the eigenbasis of U .

The parameterized circuits we used as ansätze for the diagonal unitary D and basis transformation W are shown in Fig. 3. A general diagonal unitary $D \in \text{SU}(2^n)$ on n qubits contains $2^n - 1$ variational parameters. In our experiment we implement a two-qubit version of this exact D containing 3 variables. In general an arbitrary unitary W can be constructed from any general n -qubit parameterized quantum circuit with $\text{poly}(n)$ variables. The expressive power of different options has been investigated in [69, 70]. The two-qubit circuit we use to implement the arbitrary unitary W consists of 3 layers of X , Y rotations and phase gates on each qubit, separated by 2 CNOT gates.

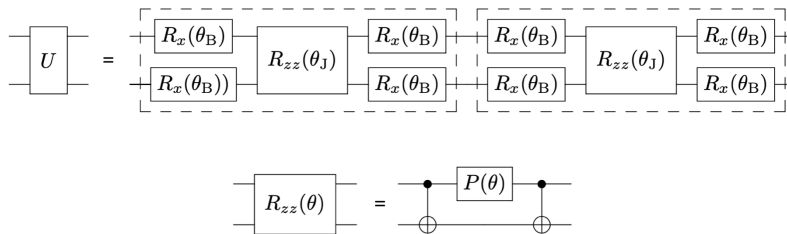


FIG. 1. **Circuit for the short-time evolution of the Ising model.** The boxes indicate individual Trotter steps. Here $R_x(\theta) = e^{i\theta X/2}$ is a single qubit Pauli X rotation, $P(\gamma) = \text{diag}(1, e^{i\gamma})$ is a single qubit phase gate and $R_{zz}(\theta) = e^{i\theta Z \otimes Z/2}$ is a two-qubit diagonal unitary.

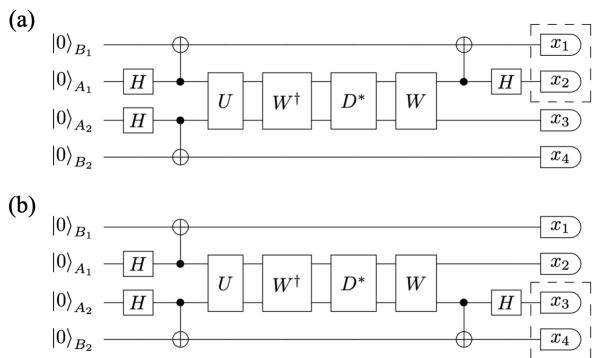


FIG. 2. **Cost function circuit.** Circuits to learn the spectral decomposition WDW^\dagger of a two-qubit unitary U on a four-qubit chain. Each cost function and gradient evaluation requires the estimation of $\text{Pr}(00)_{1,2}$ and $\text{Pr}(00)_{3,4}$, obtained by measuring the qubits in the dashed boxes of (a) and (b).

Cost function. To compile the target unitary into a diagonal form we use the local Hilbert-Schmidt test cost function defined in [38]. For learning a 4×4 unitary matrix, this cost can be written as

$$C = 1 - \frac{1}{2} (\text{Pr}(00)_{1,2} + \text{Pr}(00)_{3,4}) \quad (4)$$

where $\text{Pr}(00)_{1,2}$ and $\text{Pr}(00)_{3,4}$ are the probabilities of observing the outcome 00 on qubits (1,2) and (3,4) on running the circuits shown in Fig. 2(a) and Fig. 2(b) respectively.

The probabilities $\text{Pr}(00)_{1,2}$ and $\text{Pr}(00)_{3,4}$ are measures of the entanglement fidelity of the unitary channel UV^\dagger with $V = WDW^\dagger$. As a result, this cost is faithful, vanishing if and only if the diagonalization WDW^\dagger matches the target unitary U (up to a global phase). Furthermore, the cost is operationally meaningful for non-zero values in virtue of upper bounding the average gate fidelity between U and V . Hence a small value of C guarantees that the diagonalization WDW^\dagger is an accurate approximation of the target unitary U . We note that this cost,

Eq. (4) involves only local measures and hence mitigates trainability issues associated with barren plateaus [71–82]. For more details on the cost see Ref. [38].

Training. The parameters $(\theta_1, \dots, \theta_{18}, \gamma_1, \dots, \gamma_3)$ are initialized to minimize the cost (4) with the exchange energy J in (1) set to zero, which can be simulated efficiently and solved exactly.

The circuits are trained to minimise the cost using gradient descent. At each step of the training, we measure the cost and gradients $\frac{\partial C}{\partial \theta_k}$ and $\frac{\partial C}{\partial \gamma_l}$ at a particular point (θ, γ) in the parameter space, and use this to update (θ, γ) according to

$$\theta_k \leftarrow \theta_k - \eta \frac{\partial C}{\partial \theta_k} \quad (5)$$

$$\gamma_l \leftarrow \gamma_l - \eta \frac{\partial C}{\partial \gamma_l}, \quad (6)$$

where η is the learning rate. The gradients $\frac{\partial C}{\partial \theta_k}$ and $\frac{\partial C}{\partial \gamma_l}$ are measured using the parameter shift rule derived in Ref. [56]. In each optimization step the 21 components of the gradient are measured, requiring the measurement of 156 distinct circuits. For each cost evaluation we took 8000 measurement shots.

The learning rate was decreased as the optimization progressed according to a schedule

$$\eta(j) = \frac{\eta_0}{[1 + (j/\delta)]^\kappa}, \quad (7)$$

where $j \in \{0, 1, 2, \dots, 16\}$ is the optimization step number. The hyperparameters $\eta_0 = 1.1$, $\kappa = 0.5$, and $\delta = 12$ were optimized by classical simulation. Additional details about the training are provided in the Supplementary Information.

RESULTS

To assess the quality of the optimization, the parameters found at each step of the training were used to evaluate C both on the quantum computer and classically.

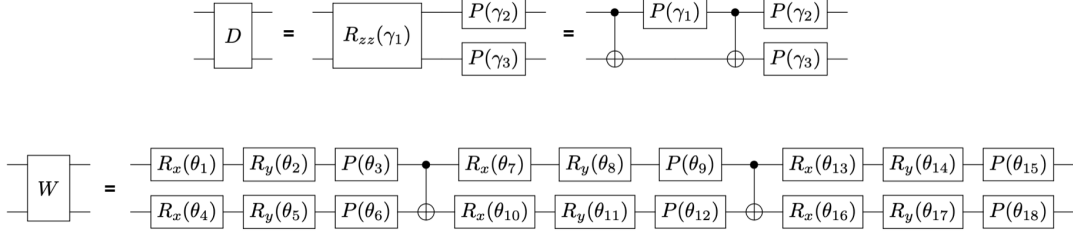


FIG. 3. **Ansatz circuits.** Implemented circuits for the diagonal unitary D and basis transformation W . Here $R_{zz}(\gamma) = e^{i\gamma Z \otimes Z/2}$ is a two-qubit diagonal unitary and $P(\gamma) = \text{diag}(1, e^{i\gamma})$ is a single qubit phase gate. D contains 3 variational parameters. W has 3 layers and 18 variational parameters.

The results are shown in Fig. 4. The classical cost, which we call the noise-free or *ideal* cost, reflects the true accuracy of the optimized circuits. We successfully reduced the raw cost to 0.1099 corresponding to an ideal cost of 0.013. The raw cost from the quantum computer is higher than the ideal cost because of gate errors.

The inset of Fig. 4 confirms that the errors in D and WDW^\dagger are both iteratively reduced as the cost is trained. Here the Frobenius distance between U and V is plotted, minimized over the arbitrary global phase $e^{i\varphi}$. The ideal and learnt diagonals are also compared, accounting for the global phase $e^{i\varphi}$ and for a possible reordering, specified by a permutation matrix χ . Specifically, we plot the Frobenius distance $\min_{\varphi, \chi} \|D_{\text{exact}} - e^{i\varphi} \chi D \chi^\dagger\|$ where D_{exact} is a diagonal matrix with $\{\lambda_i^{\text{exact}}\}$, the ordered exact spectrum of U , along the diagonal. This is equivalent to the sum of the eigenvalue errors $\sum_i |\lambda_i^{\text{exact}} - \lambda_i e^{i\varphi_{\text{opt}}}|^2$, where $\{\lambda_i\}$ is the ordered learnt spectrum and φ_{opt} accounts for the global phase shift.

It is also interesting to monitor the training by using the measured gradient \mathbf{g}_{meas} at each step to calculate the angle between \mathbf{g}_{meas} and the exact gradient simulated classically. This is plotted in the Supplementary Information. The data confirms that the optimization is correctly moving downhill in the cost function landscape.

Having learned the spectral decomposition, we use the result to fast-forward the Hamiltonian simulation of the Ising model (1) for 2 spins on `ibmq_bogota`. In this experiment we prepare an initial state $|+\rangle^{\otimes 2}$ and propagate it forward in time by both Trotterization and variational fast-forwarding (with backend circuit optimization disabled in both cases). The Trotterized evolution at times $t = K\Delta t$, is obtained by applying $K = 0, 8, 16, \dots, 96$ consecutive Trotter steps from Fig. 1. After each step we experimentally measure the fidelity of the Trotterized evolution with the perfect evolution $e^{-iHt}|+\rangle^{\otimes 2}$, which contains no Trotter error. The variational fast-forwarding evolution at time t is obtained by applying the optimized variational circuits for W^\dagger , D^* , and W to

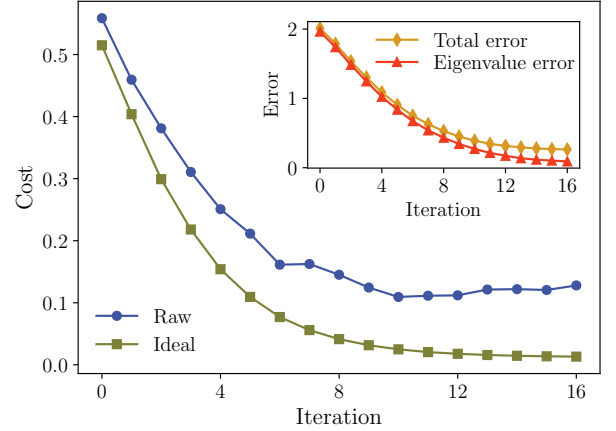


FIG. 4. **Training curves.** In the main plot we show the cost as a function of the iteration step during training. The blue curve is the measured cost function C and the green curve is its noise-free ‘ideal’ value. In the inset, the yellow curve indicates the total error in the learnt unitary defined as Frobenius distances between U and V minimized over a global phase $e^{i\varphi}$, i.e., the quantity $\min_{\varphi, \chi} \|U - e^{i\varphi} V\|$. The red curve indicates the eigenvalue error, defined as the Frobenius distance between the learnt and exact diagonal also minimized over a permutation χ , i.e., $\min_{\varphi, \chi} \|D_{\text{exact}} - e^{i\varphi} \chi D \chi^\dagger\|$.

$|+\rangle^{\otimes 2}$, but with D 's parameters $(\gamma_1, \gamma_2, \gamma_3)$ changed to

$$(\gamma_1, \gamma_2, \gamma_3) \times \frac{t}{\Delta t}. \quad (8)$$

The state fidelity with perfect evolution $e^{-iHt}|+\rangle^{\otimes 2}$ is also measured in this case. The results for this experimental fast-forwarding and experimental Trotter simulation are indicated by the green and blue solid lines respectively in Fig. 5.

We compare the experimental fast forwarding to the ideal classical fast-forwarding by also measuring the noise-free fidelities obtained by classical simulation. In this ideal simulation, the initial state $|+\rangle^{\otimes 2}$ is prepared perfectly and the Trotterized evolution includes Trotter errors but no gate errors. The measurement is also as-

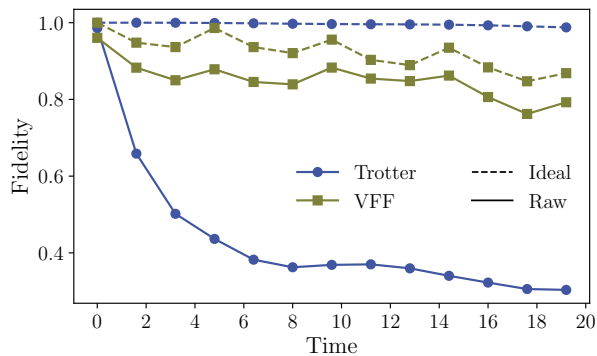


FIG. 5. **Demonstration of variational fast-forwarding.** The plot shows the measured state fidelity versus evolution time. The data (circles) are obtained at multiples of $8\Delta t$, out to $t=19.2$.

sumed to be ideal. The fidelities of these ideal simulations are indicated by the dashed lines in Fig. 5.

The ideal Trotterized evolution is nearly perfect in Fig. 5 due to the small value of Δt and use of a second-order Trotter step. The ideal variational fast-forwarding evolution is less accurate, due to the imperfect learning of U 's spectral decomposition. However, the real data taken on `ibmq_bogota` exhibits the opposite behavior. Whereas the variational fast-forwarding evolution is only slightly degraded by gate errors—because the circuit depth is independent of t —the Trotterized evolution quickly loses fidelity. Namely, while the fidelity of the variationally fast forwarded simulation remains above 0.7 for all 20 time steps, the fidelity of the Trotterized simulation is less than 0.4 after only 6 time steps. Thus Figure 5 demonstrates a striking example of fast-forwarding as well as provides further evidence that the spectral decomposition of U has been well learnt.

In conclusion, we have experimentally demonstrated the entanglement-enhanced quantum learning of a 4×4 unitary using a diagonal ansatz containing a total of 6 CNOTs and 21 variational parameters. A single input-output pair was used for training compared to the $2^2 = 4$ input-output pairs necessary for training without entangling ancillas. We both learn the unitary and its spectral decomposition, enabling the fast-forwarding of an Ising model. This four-qubit experiment took 8000 shots for each of the 156 independent circuit evaluations, at each of the 16 steps of the optimization algorithm, a total of 20×10^7 circuit evaluations. Thus, this experiment is among the most complex quantum machine learning demonstrations to date [14–20] and constitutes an important primitive in experimental quantum information science.

Acknowledgments. PJC and AS acknowledge initial support and MRG acknowledges support from LANL's Laboratory Directed Research and Development (LDRD)

program under project number 20190065DR. Additionally, PJC and AS acknowledge that (subsequent to the above acknowledged funding) this material is based upon work supported by the U.S. Department of Energy, Office of Science, National Quantum Information Science Research Centers. ZH acknowledges support from the LANL ASC Beyond Moore's Law project. We would also like to thank Andrew Arrasmith, Lukasz Cincio, and Joe Gibbs for useful discussions.

* mgeller@uga.edu

† sornborg@lanl.gov

- [1] Jacob Biamonte, Peter Wittek, Nicola Pancotti, Patrick Rebentrost, Nathan Wiebe, and Seth Lloyd, “Quantum machine learning,” *Nature* **549**, 195–202 (2017).
- [2] Aram W Harrow, Avinandan Hassidim, and Seth Lloyd, “Quantum algorithm for linear systems of equations,” *Physical review letters* **103**, 150502 (2009).
- [3] B David Clader, Bryan C Jacobs, and Chad R Sprouse, “Preconditioned quantum linear system algorithm,” *Physical review letters* **110**, 250504 (2013).
- [4] Andrew M Childs, Robin Kothari, and Rolando D Somma, “Quantum algorithm for systems of linear equations with exponentially improved dependence on precision,” *SIAM Journal on Computing* **46**, 1920–1950 (2017).
- [5] Maria Schuld and Nathan Killoran, “Quantum machine learning in feature hilbert spaces,” *Physical review letters* **122**, 040504 (2019).
- [6] Vojtěch Havlíček, Antonio D Córcoles, Kristan Temme, Aram W Harrow, Abhinav Kandala, Jerry M Chow, and Jay M Gambetta, “Supervised learning with quantum-enhanced feature spaces,” *Nature* **567**, 209–212 (2019).
- [7] Nathan Wiebe, Ashish Kapoor, and Krysta M Svore, “Quantum deep learning,” *arXiv preprint arXiv:1412.3489* (2014).
- [8] Guillaume Verdon, Michael Broughton, and Jacob Biamonte, “A quantum algorithm to train neural networks using low-depth circuits,” *arXiv preprint arXiv:1712.05304* (2017).
- [9] Abhinav Kandala, Antonio Mezzacapo, Kristan Temme, Maika Takita, Markus Brink, Jerry M Chow, and Jay M Gambetta, “Hardware-efficient variational quantum eigensolver for small molecules and quantum magnets,” *Nature* **549**, 242–246 (2017).
- [10] Abhinav Kandala, Kristan Temme, Antonio D Córcoles, Antonio Mezzacapo, Jerry M Chow, and Jay M Gambetta, “Error mitigation extends the computational reach of a noisy quantum processor,” *Nature* **567**, 491–495 (2019).
- [11] Google AI Quantum and Collaborators, Frank Arute, Kunal Arya, Ryan Babbush, Dave Bacon, Joseph C. Bardin, Rami Barends, Sergio Boixo, Michael Broughton, Bob B. Buckley, David A. Buell, Brian Burkett, Nicholas Bushnell, Yu Chen, Zijun Chen, Benjamin Chiaro, Roberto Collins, William Courtney, Sean Demura, Andrew Dunsworth, Edward Farhi, Austin Fowler, Brooks Foxen, Craig Gidney, Marissa Giustina, Rob Graff, Steve Habegger, Matthew P. Harrigan, Alan Ho, Sabrina Hong,

- Trent Huang, William J. Huggins, Lev Ioffe, Sergei V. Isakov, Evan Jeffrey, Zhang Jiang, Cody Jones, Dvir Kafri, Kostyantyn Kechedzhi, Julian Kelly, Seon Kim, Paul V. Klimov, Alexander Korotkov, Fedor Kostritsa, David Landhuis, Pavel Laptev, Mike Lindmark, Erik Lucero, Orion Martin, John M. Martinis, Jarrod R. McClean, Matt McEwen, Anthony Megrant, Xiao Mi, Masoud Mohseni, Wojciech Mruzekiewicz, Josh Mutus, Ofer Naaman, Matthew Neeley, Charles Neill, Hartmut Neven, Murphy Yuezhen Niu, Thomas E. O'Brien, Eric Ostby, Andre Petukhov, Harald Putterman, Chris Quintana, Pedram Roushan, Nicholas C. Rubin, Daniel Sank, Kevin J. Satzinger, Vadim Smelyanskiy, Doug Strain, Kevin J. Sung, Marco Szalay, Tyler Y. Takeshita, Amit Vainsencher, Theodore White, Nathan Wiebe, Z. Jamie Yao, Ping Yeh, and Adam Zalcman, "Hartree-fock on a superconducting qubit quantum computer," **369**, 1084–1089 (2020).
- [12] Frank Arute, Kunal Arya, Ryan Babbush, Dave Bacon, Joseph C Bardin, Rami Barends, Andreas Bengtsson, Sergio Boixo, Michael Broughton, Bob B Buckley, *et al.*, "Observation of separated dynamics of charge and spin in the fermi-hubbard model," arXiv preprint arXiv:2010.07965 (2020).
- [13] Igor Aleiner, Frank Arute, Kunal Arya, Juan Atalaya, Ryan Babbush, Joseph C Bardin, Rami Barends, Andreas Bengtsson, Sergio Boixo, Alexandre Bourassa, *et al.*, "Accurately computing electronic properties of materials using eigenenergies," arXiv preprint arXiv:2012.00921 (2020).
- [14] Diego Riste, Marcus P da Silva, Colm A Ryan, Andrew W Cross, Antonio D Córcoles, John A Smolin, Jay M Gambetta, Jerry M Chow, and Blake R Johnson, "Demonstration of quantum advantage in machine learning," npj Quantum Information **3**, 1–5 (2017).
- [15] Maria Schuld, Mark Fingerhuth, and Francesco Petruccione, "Implementing a distance-based classifier with a quantum interference circuit," EPL (Europhysics Letters) **119**, 60002 (2017).
- [16] Xi-Wei Yao, Hengyan Wang, Zeyang Liao, Ming-Cheng Chen, Jian Pan, Jun Li, Kechao Zhang, Xingcheng Lin, Zhehui Wang, Zhihuang Luo, *et al.*, "Quantum image processing and its application to edge detection: theory and experiment," Physical Review X **7**, 031041 (2017).
- [17] He-Liang Huang, Xi-Lin Wang, Peter P Rohde, Yi-Han Luo, You-Wei Zhao, Chang Liu, Li Li, Nai-Le Liu, Chao-Yang Lu, and Jian-Wei Pan, "Demonstration of topological data analysis on a quantum processor," Optica **5**, 193–198 (2018).
- [18] D. Zhu, N. M. Linke, M. Benedetti, K. A. Landsman, N. H. Nguyen, C. H. Alderete, A. Perdomo-Ortiz, N. Korda, A. Garfoot, C. Brecque, L. Egan, O. Perdomo, and C. Monroe, "Training of quantum circuits on a hybrid quantum computer," **5** (2019), 10.1126/sciadv.aaw9918.
- [19] Kunal Kathuria, Aakrosh Ratan, Michael McConnell, and Stefan Bekiranov, "Implementation of a hamming distance-like genomic quantum classifier using inner products on ibmqx2 and ibmq_16_melbourne," Quantum machine intelligence **2**, 1–26 (2020).
- [20] Teague Tomesh, Pranav Gokhale, Eric R Anschuetz, and Frederic T Chong, "Coreset clustering on small quantum computers," arXiv preprint arXiv:2004.14970 (2020).
- [21] M. Cerezo, Andrew Arrasmith, Ryan Babbush, Simon C Benjamin, Suguru Endo, Keisuke Fujii, Jarrod R McClean, Kosuke Mitarai, Xiao Yuan, Lukasz Cincio, and Patrick J. Coles, "Variational quantum algorithms," arXiv preprint arXiv:2012.09265 (2020).
- [22] Suguru Endo, Zhenyu Cai, Simon C Benjamin, and Xiao Yuan, "Hybrid quantum-classical algorithms and quantum error mitigation," Journal of the Physical Society of Japan **90**, 032001 (2021).
- [23] Kishor Bharti, Alba Cervera-Lierta, Thi Ha Kyaw, Tobias Haug, Sumner Alperin-Lea, Abhinav Anand, Matthias Degroote, Hermanni Heimonen, Jakob S. Kottmann, Tim Menke, Wai-Keong Mok, Sukin Sim, Leong-Chuan Kwek, and Alán Aspuru-Guzik, "Noisy intermediate-scale quantum (nisq) algorithms," arXiv preprint arXiv:2101.08448 (2021).
- [24] Jonathan Romero, Jonathan P Olson, and Alan Aspuru-Guzik, "Quantum autoencoders for efficient compression of quantum data," Quantum Science and Technology **2**, 045001 (2017).
- [25] Dmytro Bondarenko and Polina Feldmann, "Quantum autoencoders to denoise quantum data," Physical Review Letters **124**, 130502 (2020).
- [26] Carlos Bravo-Prieto, Ryan LaRose, Marco Cerezo, Yigit Subasi, Lukasz Cincio, and Patrick J Coles, "Variational quantum linear solver," arXiv preprint arXiv:1909.05820 (2019).
- [27] Xiaosi Xu, Jinzhao Sun, Suguru Endo, Ying Li, Simon C Benjamin, and Xiao Yuan, "Variational algorithms for linear algebra," arXiv preprint arXiv:1909.03898 (2019).
- [28] Hsin-Yuan Huang, Kishor Bharti, and Patrick Rebentrost, "Near-term quantum algorithms for linear systems of equations," arXiv preprint arXiv:1909.07344 (2019).
- [29] Alberto Peruzzo, Jarrod McClean, Peter Shadbolt, Man-Hong Yung, Xiao-Qi Zhou, Peter J Love, Alán Aspuru-Guzik, and Jeremy L O'brien, "A variational eigenvalue solver on a photonic quantum processor," Nature communications **5**, 4213 (2014).
- [30] Edward Farhi, Jeffrey Goldstone, and Sam Gutmann, "A quantum approximate optimization algorithm," arXiv preprint arXiv:1411.4028 (2014).
- [31] Stuart Hadfield, Zihui Wang, Bryan O'Gorman, Eleanor G Rieffel, Davide Venturelli, and Rupak Biswas, "From the quantum approximate optimization algorithm to a quantum alternating operator ansatz," Algorithms **12**, 34 (2019).
- [32] Kosuke Mitarai, Makoto Negoro, Masahiro Kitagawa, and Keisuke Fujii, "Quantum circuit learning," Physical Review A **98**, 032309 (2018).
- [33] Ryan LaRose, Arkin Tikku, Étude O'Neel-Judy, Lukasz Cincio, and Patrick J Coles, "Variational quantum state diagonalization," npj Quantum Information **5**, 1–10 (2019).
- [34] M Cerezo, Kunal Sharma, Andrew Arrasmith, and Patrick J Coles, "Variational quantum state eigensolver," arXiv preprint arXiv:2004.01372 (2020).
- [35] Carlos Bravo-Prieto, Diego García-Martín, and José I Latorre, "Quantum singular value decomposer," Physical Review A **101**, 062310 (2020).
- [36] Marco Cerezo, Alexander Poremba, Lukasz Cincio, and Patrick J Coles, "Variational quantum fidelity estimation," Quantum **4**, 248 (2020).
- [37] Jacob L Beckey, M Cerezo, Akira Sone, and Patrick J Coles, "Variational quantum algorithm for estimating the quantum fisher information," arXiv preprint

- arXiv:2010.10488 (2020).
- [38] Sumeet Khatri, Ryan LaRose, Alexander Poremba, Lukasz Cincio, Andrew T Sornborger, and Patrick J Coles, “Quantum-assisted quantum compiling,” *Quantum* **3**, 140 (2019).
- [39] Kunal Sharma, Sumeet Khatri, Marco Cerezo, and Patrick J Coles, “Noise resilience of variational quantum compiling,” *New Journal of Physics* **22**, 043006 (2020).
- [40] Tyson Jones and Simon C Benjamin, “Quantum compilation and circuit optimisation via energy dissipation,” arXiv preprint arXiv:1811.03147 (2018).
- [41] Lukasz Cincio, Yiğit Subaşı, Andrew T Sornborger, and Patrick J Coles, “Learning the quantum algorithm for state overlap,” *New Journal of Physics* **20**, 113022 (2018).
- [42] M. Horodecki, P. Horodecki, and R. Horodecki, “General teleportation channel, singlet fraction, and quasidistillation,” *Physical Review A* **60**, 1888–1898 (1999).
- [43] M. A. Nielsen, “A simple formula for the average gate fidelity of a quantum dynamical operation,” *Physics Letters A* **303**, 249–252 (2002).
- [44] Kyle Poland, Kerstin Beer, and Tobias J Osborne, “No free lunch for quantum machine learning,” arXiv preprint arXiv:2003.14103 (2020).
- [45] Kunal Sharma, M. Cerezo, Zoë Holmes, Lukasz Cincio, Andrew Sornborger, and Patrick J Coles, “Reformulation of the no-free-lunch theorem for entangled data sets,” arXiv preprint arXiv:2007.04900 (2020).
- [46] Seth Lloyd, “Universal quantum simulators,” *Science*, 1073–1078 (1996).
- [47] Andrew M Childs and Yuan Su, “Nearly optimal lattice simulation by product formulas,” *Physical review letters* **123**, 050503 (2019).
- [48] Jeongwan Haah, Matthew B Hastings, Robin Kothari, and Guang Hao Low, “Quantum algorithm for simulating real time evolution of lattice hamiltonians,” *SIAM Journal on Computing*, FOCS18–250 (2021).
- [49] Guang Hao Low, Vadym Kliuchnikov, and Nathan Wiebe, “Well-conditioned multiproduct hamiltonian simulation,” arXiv preprint arXiv:1907.11679 (2019).
- [50] Dorit Aharonov and Amnon Ta-Shma, “Adiabatic quantum state generation and statistical zero knowledge,” in *Proceedings of the thirty-fifth annual ACM symposium on Theory of computing* (2003) pp. 20–29.
- [51] Dominic W Berry, Andrew M Childs, Richard Cleve, Robin Kothari, and Rolando D Somma, “Exponential improvement in precision for simulating sparse hamiltonians,” in *Proceedings of the forty-sixth annual ACM symposium on Theory of computing* (2014) pp. 283–292.
- [52] Guang Hao Low and Isaac L Chuang, “Optimal hamiltonian simulation by quantum signal processing,” *Physical review letters* **118**, 010501 (2017).
- [53] Dominic W Berry, Andrew M Childs, Richard Cleve, Robin Kothari, and Rolando D Somma, “Simulating hamiltonian dynamics with a truncated taylor series,” *Physical review letters* **114**, 090502 (2015).
- [54] Dominic W Berry, Andrew M Childs, and Robin Kothari, “Hamiltonian simulation with nearly optimal dependence on all parameters,” in *2015 IEEE 56th Annual Symposium on Foundations of Computer Science (IEEE, 2015)* pp. 792–809.
- [55] Guang Hao Low and Isaac L Chuang, “Hamiltonian simulation by qubitization,” *Quantum* **3**, 163 (2019).
- [56] Cristina Cirstoiu, Zoe Holmes, Joseph Iosue, Lukasz Cincio, Patrick J Coles, and Andrew Sornborger, “Variational fast forwarding for quantum simulation beyond the coherence time,” *npj Quantum Information* **6**, 1–10 (2020).
- [57] Andrew Arrasmith, Lukasz Cincio, Andrew T Sornborger, Wojciech H Zurek, and Patrick J Coles, “Variational consistent histories as a hybrid algorithm for quantum foundations,” *Nature communications* **10**, 1–7 (2019).
- [58] Colin J Trout, Muyuan Li, Mauricio Gutiérrez, Yukai Wu, Sheng-Tao Wang, Luming Duan, and Kenneth R Brown, “Simulating the performance of a distance-3 surface code in a linear ion trap,” *New Journal of Physics* **20**, 043038 (2018).
- [59] Suguru Endo, Jinzhao Sun, Ying Li, Simon C Benjamin, and Xiao Yuan, “Variational quantum simulation of general processes,” *Physical Review Letters* **125**, 010501 (2020).
- [60] Yong-Xin Yao, Niladri Gomes, Feng Zhang, Thomas Iadecola, Cai-Zhuang Wang, Kai-Ming Ho, and Peter P Orth, “Adaptive variational quantum dynamics simulations,” arXiv preprint arXiv:2011.00622 (2020).
- [61] Marcello Benedetti, Mattia Fiorentini, and Michael Lubasch, “Hardware-efficient variational quantum algorithms for time evolution,” arXiv preprint arXiv:2009.12361 (2020).
- [62] Kentaro Heya, Ken M Nakanishi, Kosuke Mitarai, and Keisuke Fujii, “Subspace variational quantum simulator,” arXiv preprint arXiv:1904.08566 (2019).
- [63] Kishor Bharti and Tobias Haug, “Quantum assisted simulator,” arXiv preprint arXiv:2011.06911 (2020).
- [64] Jonathan Wei Zhong Lau, Kishor Bharti, Tobias Haug, and Leong Chuan Kwek, “Quantum assisted simulation of time dependent hamiltonians,” arXiv preprint arXiv:2101.07677 (2021).
- [65] Tobias Haug and Kishor Bharti, “Generalized quantum assisted simulator,” arXiv preprint arXiv:2011.14737 (2020).
- [66] Stefano Barison, Filippo Vicentini, and Giuseppe Carleo, “An efficient quantum algorithm for the time evolution of parameterized circuits,” arXiv preprint arXiv:2101.04579 (2021).
- [67] Joe Gibbs, Kaitlin Gili, Zoë Holmes, Benjamin Commeau, Andrew Arrasmith, Lukasz Cincio, Patrick J Coles, and Andrew Sornborger, “Long-time simulations with high fidelity on quantum hardware,” arXiv preprint arXiv:2102.04313 (2021).
- [68] Benjamin Commeau, Marco Cerezo, Zoë Holmes, Lukasz Cincio, Patrick J Coles, and Andrew Sornborger, “Variational hamiltonian diagonalization for dynamical quantum simulation,” arXiv preprint arXiv:2009.02559 (2020).
- [69] Jirawat Tangpanitanon, Supanut Thanasilp, Ninnat Dangniam, Marc-Antoine Lemonde, and Dimitris G Angelakis, “Expressibility and trainability of parameterized analog quantum systems for machine learning applications,” arXiv preprint arXiv:2005.11222 (2020).
- [70] Sukin Sim, Peter D Johnson, and Alán Aspuru-Guzik, “Expressibility and entangling capability of parameterized quantum circuits for hybrid quantum-classical algorithms,” *Advanced Quantum Technologies* **2**, 1900070 (2019).
- [71] Jarrod R McClean, Sergio Boixo, Vadim N Smelyanskiy, Ryan Babbush, and Hartmut Neven, “Barren plateaus in quantum neural network training landscapes,” *Nature*

- communications **9**, 1–6 (2018).
- [72] M Cerezo, Akira Sone, Tyler Volkoff, Lukasz Cincio, and Patrick J Coles, “Cost function dependent barren plateaus in shallow parametrized quantum circuits,” *Nature Communications* **12**, 1–12 (2021).
 - [73] Alexey Uvarov and Jacob Biamonte, “On barren plateaus and cost function locality in variational quantum algorithms,” arXiv preprint arXiv:2011.10530 (2020).
 - [74] Samson Wang, Enrico Fontana, Marco Cerezo, Kunal Sharma, Akira Sone, Lukasz Cincio, and Patrick J Coles, “Noise-induced barren plateaus in variational quantum algorithms,” arXiv preprint arXiv:2007.14384 (2020).
 - [75] Marco Cerezo and Patrick J Coles, “Impact of barren plateaus on the hessian and higher order derivatives,” arXiv preprint arXiv:2008.07454 (2020).
 - [76] Arthur Pesah, M Cerezo, Samson Wang, Tyler Volkoff, Andrew T Sornborger, and Patrick J Coles, “Absence of barren plateaus in quantum convolutional neural networks,” arXiv preprint arXiv:2011.02966 (2020).
 - [77] Zoë Holmes, Andrew Arrasmith, Bin Yan, Patrick J Coles, Andreas Albrecht, and Andrew T Sornborger, “Barren plateaus preclude learning scramblers,” arXiv preprint arXiv:2009.14808 (2020).
 - [78] Andrew Arrasmith, M Cerezo, Piotr Czarnik, Lukasz Cincio, and Patrick J Coles, “Effect of barren plateaus on gradient-free optimization,” arXiv preprint arXiv:2011.12245 (2020).
 - [79] Carlos Ortiz Marrero, Mária Kieferová, and Nathan Wiebe, “Entanglement induced barren plateaus,” arXiv preprint arXiv:2010.15968 (2020).
 - [80] Taylor L Patti, Khadijeh Najafi, Xun Gao, and Susanne F Yelin, “Entanglement devised barren plateau mitigation,” arXiv preprint arXiv:2012.12658 (2020).
 - [81] Zoë Holmes, Kunal Sharma, M Cerezo, and Patrick J Coles, “Connecting ansatz expressibility to gradient magnitudes and barren plateaus,” arXiv preprint arXiv:2101.02138.
 - [82] Edward Grant, Leonard Wossnig, Mateusz Ostaszewski, and Marcello Benedetti, “An initialization strategy for addressing barren plateaus in parametrized quantum circuits,” *Quantum* **3**, 214 (2019).

Supplementary Information for “Experimental Quantum Learning of a Spectral Decomposition”

This document provides additional details about the experimental results. In Sec. 1 we describe the on-line superconducting qubits used in the experiment and give calibration results (gate errors, coherence times, and single-qubit measurement errors) provided by the backend. In Sec. 2 we provide additional details about the circuit training.

1. QUBITS

Data was taken on the IBM Q processor `ibmq_santiago` using the BQP software package developed by Geller and colleagues. BQP is a Python package developed to design, run, and analyze complex quantum computing and quantum information experiments using commercial backends. We demonstrate the learning of a spectral decomposition using the qubits shown in Fig. S1. Calibration data supplied by the backend is summarized in Table I. Here $T_{1,2}$ are the standard Markovian decoherence times, and

$$\epsilon = \frac{T(0|1) + T(1|0)}{2} \quad (\text{S1})$$

is the single-qubit state-preparation and measurement (SPAM) error, averaged over initial states. The U_2 error column gives the single-qubit gate error measured by randomized benchmarking. The CNOT errors are also measured by randomized benchmarking.

TABLE I. Calibration data provided by IBM Q for the `ibmq_bogota` chip during the period of data acquisition.

Qubit	T_1 (μs)	T_2 (μs)	SPAM error ϵ	U_2 error
Q_0	136.6	178.0	0.056	3.70e-4
Q_1	132.3	117.4	0.045	2.01e-4
Q_2	65.4	132.4	0.024	2.48e-4
Q_3	103.6	158.3	0.020	4.74e-4
CNOT gates			CNOT error	
CNOT _{0,1}		CNOT _{1,0}	1.04e-3	
CNOT _{1,2}		CNOT _{2,1}	8.12e-3	
CNOT _{2,3}		CNOT _{3,2}	3.81e-2	

2. TRAINING

The variational circuits for W and D were trained by gradient descent

$$\begin{aligned} \theta_k &\leftarrow \theta_k - \eta \frac{\partial C_{\text{LHST}}}{\partial \theta_k} \\ \gamma_l &\leftarrow \gamma_l - \eta \frac{\partial C_{\text{LHST}}}{\partial \gamma_l}, \end{aligned} \quad (\text{S2})$$

where θ_k and γ_l are the variational parameters for the W and D circuits, respectively, and η is the learning rate. We used the variable learning rate plotted in Fig. S2a), which was optimized by classical simulation. At each step of the training, we measure the cost C_{LHST} and gradients $\partial C_{\text{LHST}}/\partial \theta_k$ and $\partial C_{\text{LHST}}/\partial \gamma_l$ at a particular point $(\theta_1, \dots, \theta_{18}, \gamma_1, \dots, \gamma_3)$ in parameter space, and use this to update $(\theta_1, \dots, \theta_{18}, \gamma_1, \dots, \gamma_3)$ according to (S2). We also calculate the angle between the measured gradient and the exact gradient simulated classically, which is plotted in Fig. S2b). This data shows that the measured gradient is correctly pointing uphill until the end of the training when a local minimum is reached and the gradient becomes small and noisy.



FIG. S1. Layout of IBM Q device `ibmq_bogota`. In this work we use qubits Q_0 , Q_1 , Q_2 and Q_3 for the training and qubits Q_1 and Q_2 for the Trotter and VFF comparison.

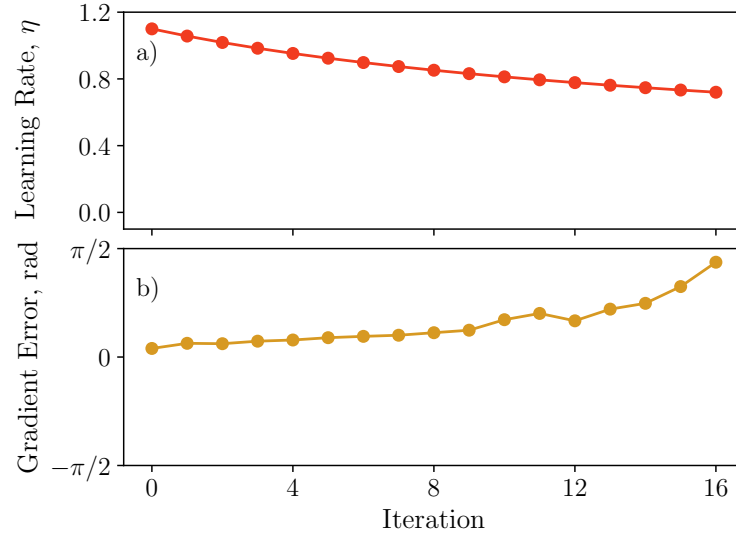


FIG. S2. (a) Learning rate versus optimization step during training by gradient descent. This rate obeys $\eta(j) = \frac{\eta_0}{[1+(j/\delta)]^\kappa}$ where $j \in \{0, 1, 2, \dots, 16\}$ is the optimization step number and the hyperparameters $\eta_0 = 1.1$, $\kappa = 0.5$, and $\delta = 12$ were optimized by classical simulation. (b) Error in the measured gradient direction during training. Here we plot the angle between gradient measured on ibmq_bogota during training, and true gradient calculating classically for the same set of parameters, for each optimization step.